Highly sensitive 26Al measurements by Ion-Laser-InterAction Mass Spectrometry

International Journal of Mass Spectrometry 465 (2021) 116576

Contents lists available at ScienceDirect

International Journal of Mass Spectrometry

journal homepage: www.elsevier.com/locate/ijms

Highly sensitive ^{26}Al measurements by Ion-Laser-InterAction Mass Spectrometry

Johannes Lachner [a, b, *], Martin Martschini [a], Andreas Kalb [a], Michael Kern [a], Oscar Marchhart [a], Felix Plasser [c], Alfred Priller [a], Peter Steier [a], Alexander Wieser [a], Robin Golser [a]

[a] University of Vienna, Faculty of Physics, 1090, Vienna, Austria
[b] Helmholtz-Zentrum Dresden-Rossendorf, 01328, Dresden, Germany
[c] Department of Chemistry, Loughborough University, Loughborough, LE11 3TU, UK

ARTICLE INFO

Article history:
Received 23 October 2020
Received in revised form
4 March 2021
Accepted 8 March 2021
Available online 18 March 2021

Keywords:
Accelerator mass spectrometry
Ion-laser interaction mass spectrometry
Laser photodetachment
Isobar suppression
26Al
AMS

ABSTRACT

The method of Ion-Laser InterAction Mass Spectrometry (ILIAMS) offers new options for the determination of ^{26}Al by Accelerator Mass Spectrometry (AMS) and improves the sensitivity and efficiency for the detection of this isotope in artificial and environmental samples. In ILIAMS, a laser is overlapped with the ion beam during its passage through a radiofrequency quadrupole ion cooler. Those ions with electron affinity lower than the energy of the photons are selectively neutralized in a photodetachment process. Because the electron affinity of MgO is lower than that of AlO, ILIAMS can suppress the isobar ^{26}Mg by 14 orders of magnitude. No further isobar suppression on the high-energy side of the spectrometer is necessary, so that the more prolific AlO^- beam can now also be used at facilities with terminal voltages < 5 MV. At the 3 MV Vienna Environmental Research Accelerator (VERA) routine ^{26}Al AMS measurements assisted by ILIAMS are performed utilizing AlO^- extracted from the ion source and charge states 2+ and 3+ for the Al ions after the accelerator on the high-energy side of the spectrometer. The most efficient generation of AlO^- currents (in the range of several μA) is realized when mixing the Al_2O_3 sample material with Fe powder. Blank materials are measured down to $^{26}Al/^{27}Al$ ratios of $5 \cdot 10^{-16}$. The efficiency relative to the use of Al^- extraction is improved typically by a factor 3–5 and thus the new method is useful for measurements with highest sensitivity and down to very low $^{26}Al/^{27}Al$ ratios.

1. Introduction

The long-lived nuclide ^{26}Al ($T_{1/2} = 717 \pm 24$ kyr [1], occurs on Earth mainly as a product of spallation reactions of the galactic cosmic rays on target atoms such as Si. Typical abundances relative to the stable isotope ^{27}Al range from $^{26}Al/^{27}Al = 10^{-15}$ to 10^{-11}. The necessary detection sensitivity can only be reached by using the method of Accelerator Mass Spectrometry (AMS) and detection limits of $^{26}Al/^{27}Al < 10^{-15}$ have been documented, e.g. by Refs. [2,3].

AMS uses negative ions that are extracted from the sample material in a Cs sputter ion source. Sputter targets prepared in the chemical extraction of Al from the original sample (e.g. rock or sediment) normally consist of Al_2O_3. Usually, they are then mixed with a metal to boost the extraction of Al^- with an electron affinity (EA) of 0.43 eV [4] from the ion source. Because of this relatively low binding energy, conventional ^{26}Al AMS measurements suffer from moderate Al^- currents (usually several 100 nA, e.g. Ref. [5] to μA [6,7]). As Mg does not form atomic negative ions, the final detection of ions at mass 26 is not affected by the isobar ^{26}Mg. Extraction of AlO^- (EA = 2.60 eV [8]) from the same target results in much higher efficiency of Al usage. In this case, the isobar ^{26}Mg is also extracted from the ion source in form of the molecule MgO^- (EA = 1.62 eV [9]) and interferes during the final detection.

The great number of applications for the radioisotope ^{26}Al has triggered efforts to improve the efficiency of the AMS measurement. Several studies dealt with the improvement of the Al^- extraction by admixing suitable metal matrices to the sputter cathodes [5,10]. Still, the prolific AlO^- molecule can give more than 10 times the beam intensity of Al^-. This approach, however, implies the need for additional isobar suppression. Methods to suppress

* Corresponding author. University of Vienna, Faculty of Physics, 1090, Vienna, Austria.
E-mail address: j.lachner@hzdr.de (J. Lachner).

https://doi.org/10.1016/j.ijms.2021.116576

the ^{26}Mg isobar were established first at large AMS facilities using full stripping of the ions ($Z(^{26}Al) = 13 > Z(^{26}Mg) = 12$) [11,12] or gas-filled magnets [13,14]. The high energies required for these isobar separation techniques are generated by selecting high charge states (e.g. 7+) after tandem accelerators with $\geq$ 8 MV terminal voltage. Still, their stripping yields for the high charge states are typically factors of 2–4 lower than for charge states <3+ at compact accelerators. Despite these losses in the detection system and in the ion transport, the better formation of AlO^- relative to Al^- leads to an improvement in the overall efficiency for ^{26}Al measurements. This is of special interest when studying low-level samples, which requires high sensitivity. The use of a gas-filled magnet was also tested at a medium-sized (6 MV terminal voltage) accelerator [15]: With a good chemical preparation, i.e. very small amounts (ppm range) of Mg being present in the final sputter sample, an improvement in efficiency by a factor of 5 could be reported.

Summarized and simplified, the two available alternatives for ^{26}Al measurements are: 1) measurements at larger facilities with higher sensitivity using AlO^-, or 2) measurements using Al^- at compact facilities, that are more readily available, straightforward to operate and allow for high transmission through the accelerator with a simple detection by counting in a gas ionization chamber.

The method of Ion-Laser-InterAction Mass Spectrometry (ILIAMS) aims at combining the best of both worlds, the high ionization yield of AlO^- and the high transmission for low charge states. Regarding the separation of the isobars, ILIAMS makes use of their different electron affinities. Inside the ion cooler, the atomic or molecular anions can be neutralized by detaching the surplus electron or the anions are transformed into another compound. In order to detach the electron or to break a charged molecule into a neutral and a charged part, sufficient energy has to be introduced into the system, e.g. via collisions with particles or absorption of photons. For the chemical transformation, a suitable chemical reaction partner, e.g. an oxygen or fluorine containing compound, has to be present. A separation of the isobars is realized if only the interfering isobar is subject to the neutralization or transformation. In the case of photodetachment, the monoenergetic laser photons can transfer a well-defined energy to the system. This simplifies predictions about the anions suitable for the purpose of ILIAMS if the relevant (adiabatic) electron affinities are known. As shown in a proof-of-principle setup [16], MgO^- can be neutralized while leaving macroscopic amounts of AlO^- unaffected. In the following, we describe the implementation of ILIAMS for measurements of ^{26}Al at the Vienna Environmental Research Accelerator (VERA).

2. Methods

The ILIAMS setup is part of the injector beam line to the accelerator and therefore is compatible with the use of accelerators of different terminal voltage. The technique and setup are described in Refs. [16,17]; first data on the realization in combination with AMS and its use as the established AMS method for ^{36}Cl detection at VERA are presented in Ref. [18] (including a schematic of the setup as used in this study) and [19].

The main principles of the ILIAMS setup installed at the VERA facility are repeated here in short form: Negative ions are produced in atomic and molecular form in the Cs sputter ion source and selected by mass in a 90° bending magnet. The following ILIAMS setup is on a high-voltage platform, so the selected anions are decelerated electrostatically to ca. 60 eV. On that platform, the ions are further cooled by collisions with a buffer gas (typically He) and are transported for nearly 1 m inside the radiofrequency quadrupole (RFQ) ion cooler. A low guiding voltage helps in pushing the ions towards the exit aperture. Within the time of their passage through the system, the ions can be overlapped with a collinearly injected laser beam.

The experiments described here make use of a frequency-doubled Nd:YVO_4 laser (λ = 532 nm, VERDI-V18, Coherent) with maximum output power of 18 W. This laser delivers 2.33 eV photons and is suitable to suppress the isobar MgO^- (EA = 1.62 eV) via photodetachment while AlO^- (EA = 2.60 eV) remains unaffected.

A perforated metal sheet can be automatically inserted in the beam path between the ion source and the first magnet and provides a reduction of the beam intensity by a factor of 60 without affecting the phase space of the ion beam [19]. This attenuator is helpful during the tuning of the stable beam and necessary for the normalization of the rare ions to the abundant beam in routine measurements. No alteration of this reduction factor, e.g. by degradation of the used perforated metal sheet, is observed over the time scale of a beamtime, which typically lasts a week.

The negative ions are reaccelerated and directed towards VERA, where further mass selection and ion detection takes place [2]. On the central high-voltage platform of the accelerator (up to 3 MV at VERA) the ions are positively charged and reach total energies of several MeV. On the high-energy side the positive ions are analyzed by mass over charge and the intensity of the radioisotope beam is recorded via counting individual events in a simple gas ionization chamber (GIC) [20].

3. Results

3.1. Improved measurement efficiency by higher ion source output using AlO^-

The intensity of the ion beam currents extracted from the AMS Cs sputter ion source is affected by the metal matrix mixed to the Al_2O_3. Tests for the optimal output of AlO^- were conducted using matrices of Ag, Cu, Fe, and Nb metal powders. The cathodes contained a known amount of Al_2O_3 ($\approx$2 mg) and were sputtered for 5–7 h, which represents long sputter durations during a measurement aiming at consuming most of the sample material. For each mixture (1:1, 1:2, or 1:3 by weight) three or more targets were prepared in Cu sample holders. Their output current was monitored in consecutive and continuous mass scans of the magnet after the ion source. The mass scans were conducted at a constant magnetic field by adjusting the high voltage potential of the ion source. The presented data were recorded in two experiments at two different magnetic fields to allow for mass scans in the range from 26 amu to 45 amu and from 41 amu to 67 amu. A mass scan is repeated three times on a cathode. This way, the material is in the ion source for about 10 min before we change to the next target. The individual targets are measured in several turns of the wheel simulating the conditions of a real measurement. By recording currents over the whole range of the mass scan it is possible to gain information on interfering anions, e.g. identifying the $^{54}Fe^-$ part at m = 54 amu ($^{27}Al_2^-$) from the recorded $^{56}Fe^-$ intensity. This way, we can conclude that >90% of the beams at 27 amu, 43 amu, 54 amu and 59 amu actually contain Al. The efficiency of ion formation is derived from the number of Al extracted as anions relative to the total number of Al atoms in the sample (Fig. 1).

Mixtures with little additional material (i.e. 1:1 by weight) dilute the Al_2O_3 to a lesser extent and thus lead to high currents and efficiencies of AlO^- extraction for all materials. An Fe matrix enhances the AlO^- yield by ca. 50% compared to the other mixtures (Fig. 1 a). All mixtures provided AlO^- currents that typically amounted to 1–4 μA. This is an increase by a factor 25–30 when compared to extracting of Al^-, for which typically 40–120 nA were measured during these tests (Fig. 1 c). The AlO^- output did not show any short-timed variations. This compares well to previous

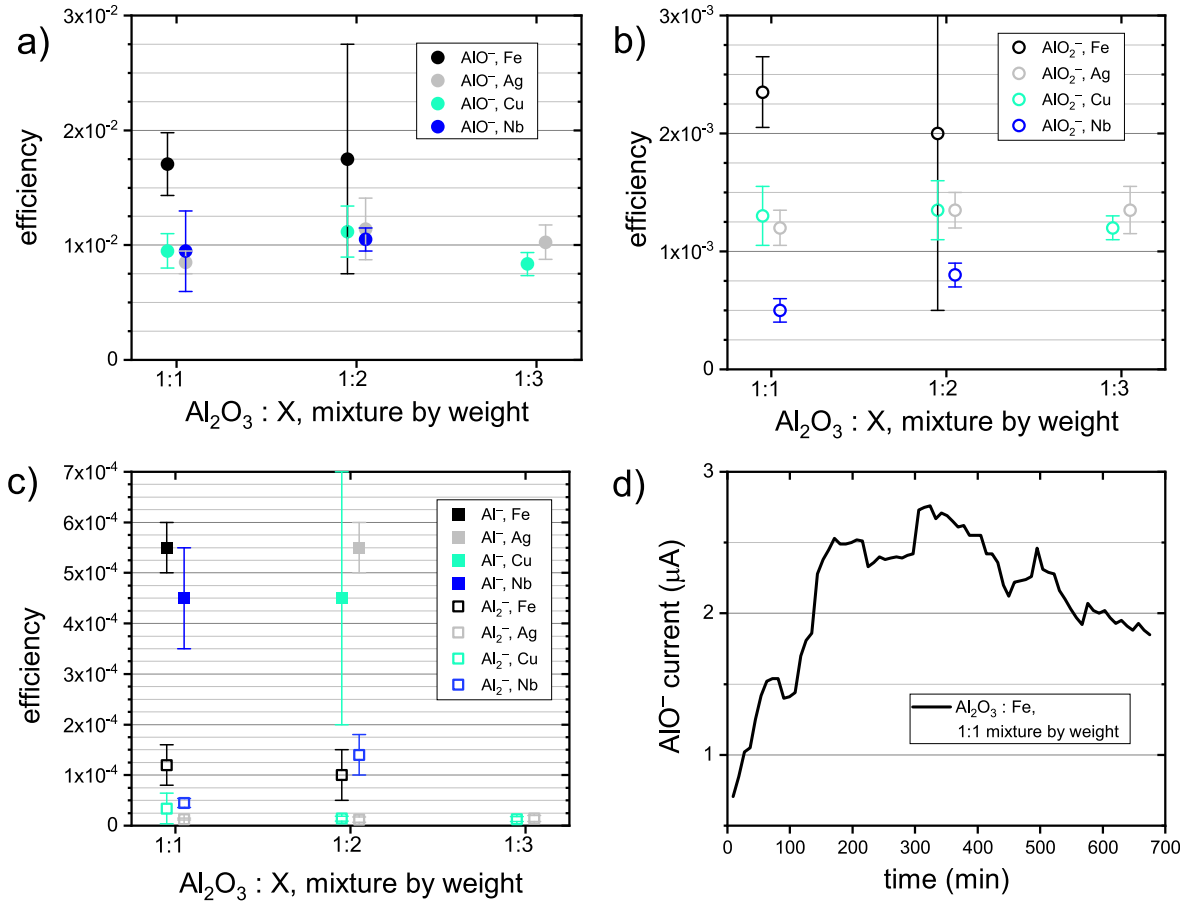

Fig. 1. Efficiency of Al anion formation for the species AlO^- (part a), AlO_2^- (part b), Al^- and Al_2^- (part c) with metal matrices Fe, Ag, Cu, Nb in different mixing ratios. Part d depicts the development of the AlO^- current for a set of Al_2O_3 and Fe mixed samples.

studies where similar outputs were found by mixing Al_2O_3 with Ag and Cu [11,14].

In addition to AlO^- and Al^-, we also checked other molecules containing Al and found AlO_2^- currents in the range of several 100 nA and Al_2^- only yielding single nA (Fig. 1 b c). Further tests using Al metal powder resulted only in AlO^- currents of several 10 nA. For most experiments described in the following, Al_2O_3 was mixed with Fe metal powder in a 1:1 wt ratio.

3.2. Beam transport through the ion cooler: isobar suppression with ILIAMS

The transmission of negative molecules is influenced strongly by the settings of the ion cooler. Being a molecular isobar system, the pair of AlO^- and MgO^- shows some pronounced features of isobar suppression in an ion cooler in addition to the effects expected from laser photodetachment. Generally, the adiabatic electron affinity is defined [21] as the transition energy from the ground vibrational/rotational state of the anion to the ground vibrational/rotational state of the neutral. In the simpler situation of atomic anions (e.g. Cl^-, S^-, Cu^-, I^-) only the ground state of anion and the ground state of neutral are relevant, whereas for the molecular anions additional breakup reactions into a charged and neutral fragment have to be considered. These reactions may already be stimulated at energies below the adiabatic electron affinity.

Quantum-mechanical calculations of the dissociation process were performed for the AlO and MgO anion. The potential energy curves were computed to model the energy profile of the dissociation of MgO and AlO in their neutral and anionic states. These computations were performed using the uncontracted multireference configuration interaction (MRCI) method [22,23] in connection with the Pople extensivity correction [24] and the ANO-L-VTZP basis set [25]. The orbitals were optimized using a complete active space self-consistent field computation with 8 (MgO), 9 (MgO^- and AlO) or 10 (AlO^-) electrons distributed in 8 orbitals. MRCI computations used the same active space as a reference space and included single and double excitations out of this space. The Columbus program system [26,27] in conjunction with integrals generated by Molcas [28] was used.

These estimations predict that for MgO^- the separation of one e^- at the equilibrium geometry is energetically favorable over the dissociation into a neutral and a charged fragment (Fig. 2a). The estimations give a value close to the electron affinity of 1.6 eV for the transformation of MgO^- into the singlet state of MgO + e^-. The dissociation of the MgO^- molecule into a neutral and a charged fragment, i.e. Mg + O^-, requires a higher energy of 2.8 eV. In comparison, the potential well of the AlO anion is much deeper (Fig. 2b) and the dissociation energy is 6.3 eV.

In the experiment the transmission of MgO^- reacts sensitively to the settings of the ion cooler. The transport of MgO^- is improved with rather short residence times inside the ion cooler and fewer interactions with the buffer gas. The residence time and the number of collisions can be regulated by changing the pressure of the buffer gas and the strength of the longitudinal field guiding the ions through the ion cooler. A successful suppression of the isobar ^{26}Mg therefore is provided by transporting the ions for a rather long time

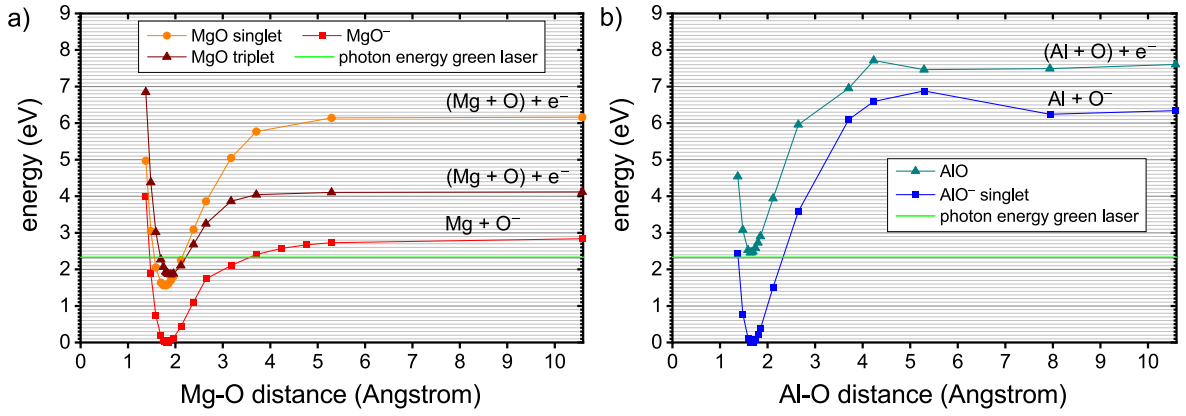

Fig. 2. a) Potential energy curves for the MgO anion and the neutral molecules in singlet (paired spin) and triplet (parallel spins) state with detached electron. Photons with an energy of 2.33 eV can initiate a detachment to the singlet or the triplet state. b) Potential energy curves for the AlO anion and the neutral molecule state with detached electron. The photon energy of 2.33 eV is not sufficient for a detachment reaction.

through the ion cooler, i.e. using a low voltage for the guiding field (Fig. 3), and allowing for a high number of collisions, i.e. increasing the pressure of the buffer gas (Fig. 4). We interpret this behavior as a more sensitive reaction of MgO^- to collisions than is the case for AlO^-, which is indicated by the results of the potential curves for the AlO and MgO anions and neutral molecules that predict a lower threshold for the dissociation of the MgO anion. The strong decrease of ^{27}Al at higher guiding field is largely due to ion optics. Interestingly, increased survival rates of ^{26}Mg at high guiding field strengths outweigh ion optical losses at these settings. The process of collisional detachment of the isobar can be further supported by admixing heavier components to the buffer gas. However, heavier components in the buffer gas also destroy a larger fraction of the AlO^- ions in collisions and less than 10% of the AlO^- are transmitted when using an admixture of O_2 to the He buffer gas. In the normal operation of the ILIAMS setup for ^{26}Al AMS, the further suppression of the MgO^- therefore is achieved by photodetachment using 532 nm photons as the photons leave the AlO^- ions unaffected.

Usually 70% of an AlO^- beam (at intensities below 100 nA) is transmitted when using pure He as buffer gas. A fraction of the beam is lost at the entrance aperture of the ion cooler as a consequence of the Coulomb repulsion between the slowed down ions that blows up the size of the beam. Furthermore, part of the AlO^- ion beam is neutralized in collisions with residual gas during the injection and extraction phase when the ions have energies in the keV range. The negative effect on the transmission is stronger for intense beams with several 100 nA or more [19].

A mass analysis of the extracted beam when injecting anions at mass 43 ($^{27}AlO^-$), mass 40 ($^{24}MgO^-$) and mass 41 ($^{25}MgO^- + {}^{24}MgOH^-$) shows oxygen anions ($O^-$, OH^- and O_2^-) leaving the ion cooler with clearly the highest OH^-/O^- ratio from mass 41. None of these species appear when injecting Cl^-. Our interpretation is that losses of the species at mass 40, 41 or 43 are, thus, to a large extent caused by collisional breakup of the injected molecular anions into neutral and charged fragments or by transformations (in the case of OH^- appearance). Possible impurities in the residual gas seem to play only a minor role [18].

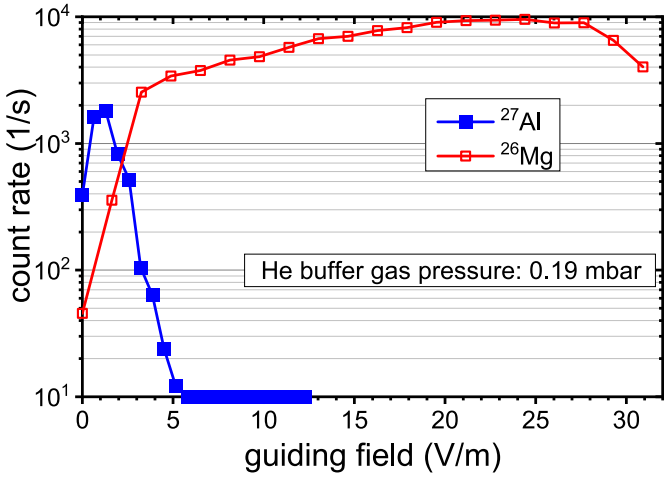

Fig. 3. The rate of events recorded in the final GIC for ^{26}Mg (red) and ^{27}Al (blue) shows different behavior depending on the strength of the guiding field that assists the transport of negative ions through the ion cooler. Measurements were performed at a He buffer gas pressure of 0.19 mbar. This is 20% lower than the typical pressure for operation of ILIAMS and gives a higher Mg count rate allowing for a fast scan of the electric field and still yielding sufficient counting statistics. $^{26}AlO^-$ or attenuated $^{27}AlO^-$ (<100 nA) beams typically require field strengths < 5 V/m depending on the settings of the injection into the ion cooler, which was kept constant during the experiment. Here, the intensity of the $^{27}AlO^-$ beam was adjusted to a level processible by the GIC by a combination of attenuators in front of the ion cooler and by detuning the injection lens in front of the accelerator (thus affecting the beam shape only after the ion cooler).

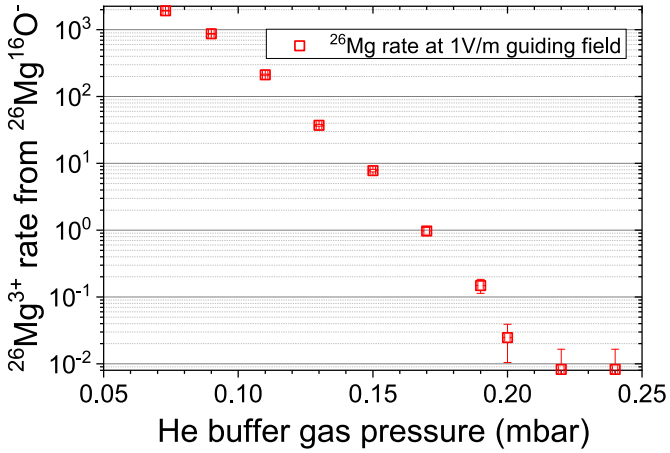

Fig. 4. The reduction of transmission for MgO^- ions through the RFQ ion beam cooler with increasing He buffer gas pressure (measured at the buffer gas inlet) shows roughly exponential behavior. For gas pressures above 0.25 mbar no event was detected during the measurement time. Instead, a limit was estimated assuming a single event.

Table 1
Figures of merit for 2+ or 3+ charge state in ILIAMS assisted ^{26}Al AMS in routine measurements of unknown samples.

charge state	stripper medium	terminal voltage	accelerator transmission	normalization factor	^{26}Al/^{27}Al blank value
2+	O_2	2.7 MV	40%	0.75	$(5 \pm 1)\cdot 10^{-16}$
3+	Ar	2.9 MV	27%	0.62	$(5 \pm 2)\cdot 10^{-16}$

The intensity of the injected ion current has an effect on the residence times inside the ion cooler and on the intensity of the transmitted beam [16]. This effect would produce a current dependency of the observed ^{26}Al/^{27}Al ratio as the transmission of the intense (μA) m = 43 amu beam would vary more with the ion current than the transmission of the rare isotope beam at m = 42 amu. The phase space conserving beam attenuator reduces the intensity of the $^{27}AlO^-$ beam by a factor of 60 to levels of several 10 nA. At these reduced intensities, the ion beam can be transported through the ion cooler without notable effect on the final ^{26}Al/^{27}Al determination. The overall beam intensity at m = 42 amu that is injected into the ion cooler can amount to single nA, which is dominated by molecular interferences such as C_2O^- or C_2HO^- rather than by $^{26}MgO^-$. We have not observed negative effects on the $^{26}AlO^-$ transmission if other ion beams at such intensity are injected simultaneously. The ^{26}Al count rate is normalized to the attenuated ^{27}Al current using a normalization factor derived from the analysis of reference materials. This normalization factor is smaller than 1 (representative values given in Table 1). The losses of ^{26}Al beam thus are higher than for the attenuated ^{27}Al beam. A small fraction of these losses can be attributed to different measurement positions of ^{26}Al in the GIC and ^{27}Al in the Faraday cup on the high-energy side of the spectrometer, the rest has to be assigned to yet unknown differences in the beam transport for the 42 amu and the attenuated 43 amu beam. The reference materials, however, show no dependency of the determined ^{26}Al/^{27}Al ratio on the ^{27}Al intensity. The slow sequential injection of the beams for ^{27}Al and ^{26}Al measurements that is required due to the insertion of the perforated metal sheet critically limits the achievable precision as variations of the sample output on time scales shorter than minutes are not appropriately reflected in the measurement. Thus, for samples with ratios above 10^{-12} data with higher precision can be expected by an Al^- measurement.

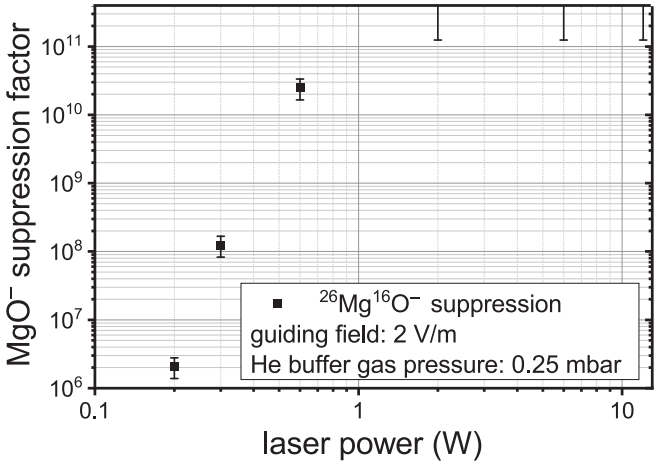

Fig. 5. The MgO^- suppression factor is recorded in measurement runs of 10 s at different laser powers and optimal conditions for AlO^- transmission through the cooler. No event was detected for P_{inj} > 1 W during the measurement time. For the estimation of the limit a single event was assumed instead.

As the molecular isobar MgO^- is already suppressed by ca. 5 orders of magnitude in the simple passage through the He filled ion cooler, requirements for additional suppression via photodetachment are slightly less stringent than in the case of S^- vs Cl^-, where photodetachment is the sole means and improves the suppression by 11 orders of magnitude [19]. Still, the gain in suppression when using the 532 nm laser is remarkable. In combination of collisional detachment and photodetachment ILIAMS achieves suppression factors > 10^{10} with a photon rate of ≈ $2\cdot10^{18}$ s^{-1}, corresponding to a laser power less than 1 W (Fig. 5). This suppression is usually sufficient for the measurement of samples produced from natural materials by the established chemical procedures for AMS, i.e. containing only ppm levels of Mg in the final Al_2O_3 sputter target. Long term measurements on samples consisting of MgO, Al_2O_3 and Fe mixed in a 1:1:1 ratio by weight suggest a suppression factor of 10^{14} using an injected laser power of 12 W. This documents that even in samples containing a substantial amount of the isobar ^{26}Mg a successful measurement of ^{26}Al can be performed. ILIAMS thus is capable of completely solving the isobaric problem for ^{26}Al measurements when working with AlO^- beams and reduces the dependency on chemical purification.

3.3. Transmission through the accelerator

Optimal conditions for ^{26}Al measurements require efficient transport through the accelerator. When ILIAMS is applied, the accelerator may not need to generate the highest ion energies for atomic isobar suppression. Instead, it is needed because the stripping process at the high voltage terminal is the most robust way to suppress any molecular interferences with m = 42 amu that survive the ion cooler.

Compared to the injection of atomic ions a worse ion optical transmission after breakup of the AlO molecule in the Coulomb explosion has to be expected. We performed measurements on the fraction of ions in the charge states Al^{1+}, Al^{2+}, Al^{3+}, and Al^{4+} relative to the injected AlO^- intensity for the stripper gases He and Ar at different terminal voltages of the accelerator. In these experiments the gas pressure inside the stripper canal was varied. As described by Ref. [29] extrapolations to 0 gas pressure give a lower limit for the actual charge state distribution. The charge state distribution extracted from our data shows no major differences between He and Ar (Fig. 6). Also single measurements performed with O_2 have so far not resulted in significantly different charge state yields. The sum of those charge state fractions does not add up to 100% as neutral particles, negative ions, and states >4+ are not included and because of ion optical and scattering losses.

The optimal charge state for the ion transport at VERA turns out to be the 2+, which reaches ion yields >50%. At the maximum terminal voltage of 3 MV, Ar shows a higher yield for the 3+ charge state, while He shows higher yields for the 1+ charge state at voltages >2 MV.

Increased stripper densities reduce the transmission because of scattering processes. The extrapolated charge state yield is a factor of 1.1–1.4 higher than the maximum transmission actually achieved for the charge states >1+ (examples in Table 1). In charge state 1+ elevations over the reported value are possible at low stripper gas pressures, where no equilibrium between the charge states is reached. If suppression of molecular interferences in charge states 1+ and 2+ requires increasing the stripper gas density, the achievable transmission through the accelerator is further decreased.

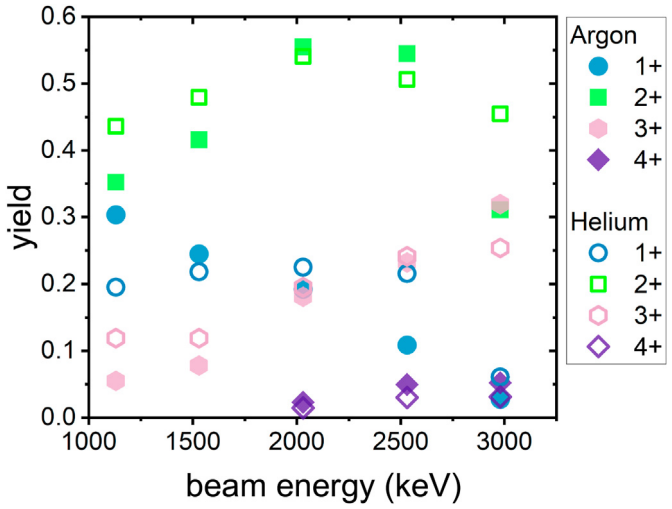

Fig. 6. Optimal charge state yields for positive charge states of Al after passage through the stripper gas. Effects of inelastic scattering were corrected by extrapolating measurement values to zero stripper gas density. At lower terminal voltages optimal conditions for the transmission required an elaborate fine-tuning of the beam.

3.4. Ion detection in gas ionization chamber for charge states 1+, 2+, 3+

On the high-energy side of the VERA AMS system the ions are filtered by a 90° bending magnet and a 90° electrostatic analyzer. The measurement of the positive ^{27}Al beam is conducted in an offset Faraday cup after the magnet. The final detection and identification of the ions with m = 26 amu takes place in a simple dual-anode gas ionization chamber (GIC) [20].

Any separation of ^{26}Mg and ^{26}Al in the GIC allows for an additional check of the ILIAMS isobar suppression. Other disturbing species reaching the detector stem from ions that form molecules with m = 42 amu on the low energy side of the spectrometer and that have the same m/q as ^{26}Al on the high-energy side.

A clean beam of atomic ions is transported to the GIC if the charge state 3+ is selected after the accelerator (Fig. 7). In this case, no m/q interferences appear in the detector at the correct m = 26 amu settings. Events counted in the GIC can be either attributed to $^{26}Mg^{3+}$ or to $^{26}Al^{3+}$. Al has the higher proton number and loses more energy than Mg in the region of the first anode and less in the second part of the GIC corresponding to different signal heights recorded on the two anodes. With this slight separation of the isobars the suppression of ^{26}Mg with ILIAMS can be monitored during the data evaluation by setting a region-of-interest in the 2D spectrum on the region where no $^{26}Al^{3+}$ should appear.

The selection of the 2+ charge state for ^{26}Al after the accelerator offers the highest yield in the transport of the beam from the low-energy side of the accelerator to the high-energy side. However, in this case interferences from surviving and broken up molecules appear in the GIC (Figs. 8 and 9).

The isobar $^{26}Mg^{2+}$ is still observably shifted relative to ^{26}Al in the 2D spectrum despite the lower beam energy. Four additional interferences can be identified in the spectrum. They are injected as m = 42 amu into the accelerator and can pass the filters on the high-energy side either as molecules in the 2+ charge state or as m/q interference. The fragments originate from molecules of $^{10}BO_2$ (EA = 4.46 eV [30], $^{13}C_2O$ (EA = 2.29 eV [31], or $^{13}C^{12}CHO$ (EA = 2.35 eV [32]. Single appearances of ^{10}B and ^{16}O occur if BO^{2+} molecules reach the detector, break up in the entrance foil and if one of the fragments is scattered in this Coulomb explosion in such way that it is not detected in the GIC. Real coincidences of ^{10}B and ^{16}O cannot be distinguished from the more intense real coincidences of two simultaneous ^{13}C events. These may reach the detector either as an intact $^{13}C_2^{2+}$ molecule or as the $^{13}C^{1+}$ fragments of the same initial $^{13}C_2O^-$ molecule broken up in the stripper canal.

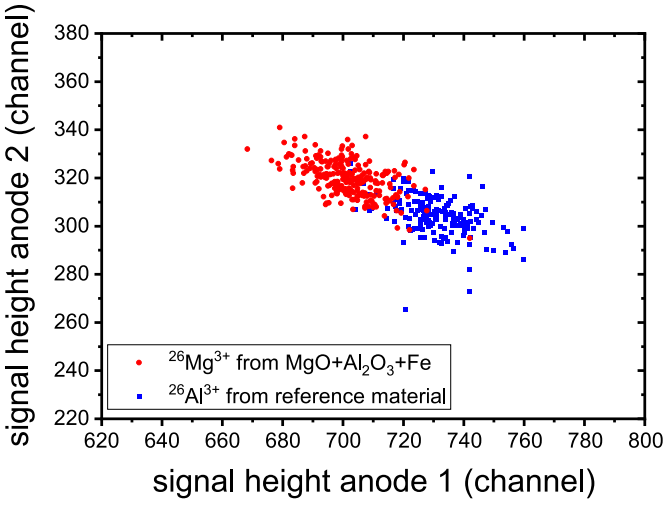

Fig. 7. The 2D spectra were recorded in the dual-anode GIC for a ^{26}Al reference material (blue) and a Mg spiked blank sample (red). Only partial suppression of Mg via ILIAMS was employed during the measurement of the Mg spiked sample.

The most intense interference stems from the single events of $^{13}C^{1+}$. These events stem either from the breakup of a $^{13}C_2O^-$ or from $^{13}C^{12}CHO^-$. The electron affinity of those molecules is similar to the photon energy of 2.33 eV used in our experiments. However, close to this threshold the cross sections for photodetachment are still low, so even in the case of C_2O^- interference a full suppression cannot be expected when using ILIAMS with 532 nm photons. Thus, for real samples produced from environmental materials, the molecular interferences may be very intense, especially the m/q interference ^{13}C. An increase in the stripper gas density breaks up the molecules more reliably and reduces the count rate for the m/q

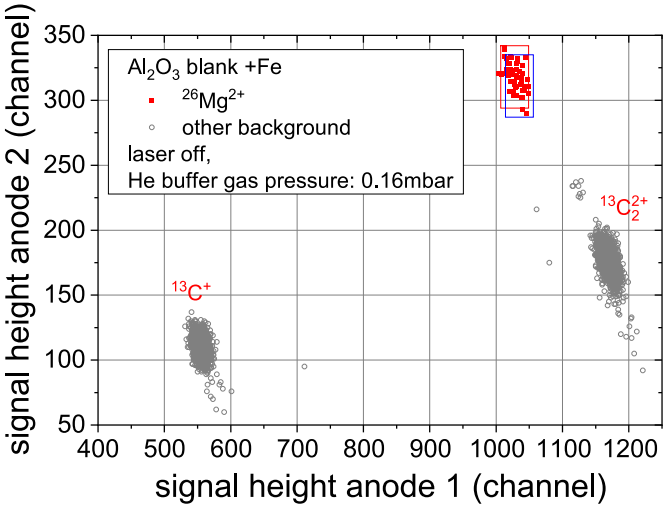

Fig. 8. The 2D spectrum from a sample with substantial Mg content shows $^{26}Mg^{2+}$ events if the ion cooler set to non-optimal conditions for Mg suppression (i.e. buffer gas pressure lowered and laser turned off). The red box indicates the region of interest for $^{26}Mg^{2+}$. Additional events are visible from the m/q interference $^{13}C^+$ and the real pile-up from two $^{13}C^+$ events or a surviving $^{13}C_2^{2+}$ molecule. The ^{26}Al region of interest is indicated in blue.

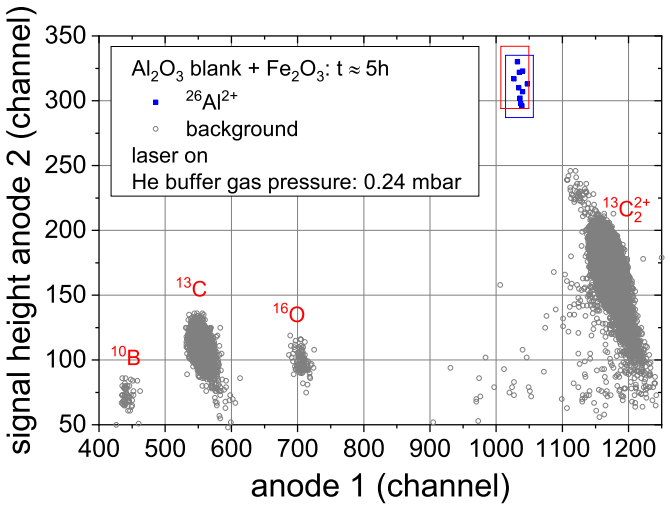

Fig. 9. The 2D spectrum was recorded over 5 h for a sample with no expected ^{26}Al content and with the ion cooler set to optimal conditions for Mg suppression. The events recorded in the region of interest for $^{26}Al^{2+}$ (blue box) result in a ratio of $^{26}Al/^{27}Al=(6 \pm 2)\cdot 10^{-16}$. In this long term measurement, additional events are visible from the m/q interference $^{13}C^{+}$ and the real pile-up from two $^{13}C^{+}$ events or a surviving $^{13}C_2{}^{2+}$ molecule and from the breakup of a $^{10}B^{16}O$ molecule. The red box indicates the region of interest for $^{26}Mg^{2+}$.

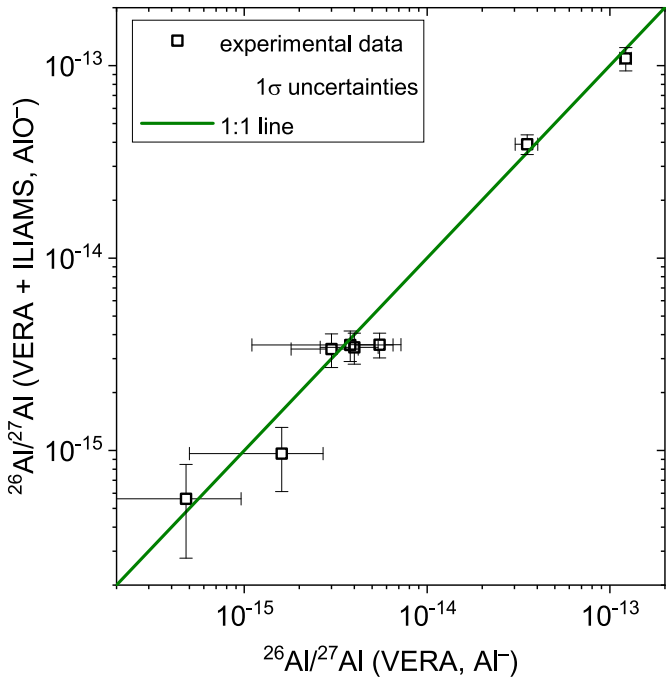

Fig. 10. Eight unknown samples spanning ratios from 10^{-16} to 10^{-13} were measured using both the conventional Al^{-} technique and the AlO^{-} method. The ratio of $(^{26}Al/^{27}Al)_{conv}/(^{26}Al/^{27}Al)_{ILIAMS}$ is consistent with unity at a $\chi^2_{red}<1$.

interference and the light molecular fragments. Still, in some cases this turns out to be insufficient as the high count rates affect the performance of the GIC through pulse pile-up and dead time. In this case, measurements have to be conducted in the 3+ charge state instead, where no molecular interferences disturb the measurement but at reduced stripping yield. An alternative could be the application of photons with slightly higher energy (e.g. $\lambda = 491$ nm) and thus destroying the molecules efficiently in the ion cooler. Also the feasibility of a SiN foil stack absorber in front of the GIC like for ^{10}Be [33] to suppress the ^{13}C interference, similar to the already practiced method of a gas absorber at lower terminal voltage for Al^{2+}-C^{1+} separation [34,35], should be explored.

For a clean Al_2O_3 blank material only events are detected that are in the ^{26}Al region of interest, i.e. shifted relative to the Mg^{2+} events. The low final ratio supports the interpretation that no MgO^{-} survives the isobar suppression in the ion cooler and contributes to the ^{26}Al events detected for this sample. This leads to low blank ratios for the ILIAMS assisted ^{26}Al AMS measurements (Table 1). Measurements performed for a set of unknown samples with ILIAMS at VERA showed consistent results in both charge states (2+,3+). Furthermore, the comparison of the combined results of the ILIAMS measurements in the two charge states with ratios measured by the conventional Al^{-} technique (Fig. 10) did not show any systematic offsets between the two methods.

The use of $^{26}Al^{1+}$ is of interest at more compact facilities than VERA with maximum accelerator voltages of 1 MV or below. In this case, the 1+ could be the most populated charge state after the accelerator. Similar to the 2+ charge state, interferences may arise from undestroyed $^{13}C_2{}^{+}$ or $(^{13}C^{12}CH)^{+}$ molecules. On the other hand, m/q interferences in other charge states are virtually impossible. The problem of molecular interferences can be solved by increasing the pressure of the stripper gas [36]. However, the corresponding reduction in transmission of the Al^{1+} beam to the detector can make the use of the 1+ charge state less sensitive than the 3+ charge state for facilities that can reach accelerator voltages ≥ 3 MV. An additional suppression of the molecular interferences via ILIAMS, e.g. by using photons with a wavelength between 480 nm and 525 nm, would be favorable also for the 1+ charge state.

4. Conclusion

This work reports on the improvement of a highly sensitive method of quantifying ^{26}Al. The gain in output using AlO^{-} instead of Al^{-} from Al_2O_3 samples is robust for different metal mixtures. The admixture of Fe metal powder showed the best effect. Improvements in beam intensity by a factor of 10 compared to Al^{-} can be realized this way. This gain is partially reduced by beam losses in the transport through the ion cooler and by a slightly worse transmission of the beam through the accelerator due to the molecular breakup in the stripping process. The isobaric interference of ^{26}Mg is totally suppressed in a combination of photodetachment and collisional detachment in the RFQ ion cooler. Quantum-chemical estimations show that not only the electron affinity of MgO is lower than that of AlO but also the dissociation energy. This might explain why the MgO^{-} breaks up more readily leading to the significant suppression of MgO^{-} in the ion cooler. To some part the MgO^{-} is also transformed into other molecules as we observed the appearance of OH^{-} and $O_2{}^{-}$ compounds after the ion cooler. While by choosing the 2+ charge state for detection of ^{26}Al a higher yield in the stripping process can be achieved, this suffers from the m/q interference from $^{13}C^{+}$ being present as single ions or as real double coincidences. At VERA with ILIAMS the optimal charge state after the accelerator to suppress any background remains the 3+. In any case, the overall efficiency of detection can be improved by a factor 3–5 relative to Al^{-}. This is an advantage for sensitive measurements that can be performed to a $^{26}Al/^{27}Al$ level even below 10^{-15}. The reliability of this method has been successfully tested for different sets of environmental samples and ILIAMS-assisted measurements are now an established ^{26}Al AMS technique at VERA. Photons of higher energy that also clean the beam of some molecular interferences are expected to improve the situation for both charge states 1+ and 2+. This way, ILIAMS also has the potential to improve the efficiency and sensitivity of ^{26}Al measurements at more compact AMS facilities.

Author statement

Johannes Lachner: Conceptualization, Methodology, Formal analysis, Investigation, Visualization, Writing – original draft, Martin Martschini: Conceptualization, Methodology, Formal analysis, Investigation, Writing – review & editing, Andreas Kalb: Investigation, Michael Kern: Validation, Investigation, Writing – review & editing, Oscar Marchhart: Validation, Investigation, Writing – review & editing, Felix Plasser: Investigation, Writing – review & editing, Alfred Priller: Investigation, Peter Steier: Software, Data curation, Writing – review & editing, Alexander Wieser: Validation, Investigation, Writing – review & editing, Robin Golser: Conceptualization, Supervision, Funding acquisition.

Declaration of competing interest

The authors declare that they have no known competing financial interests or personal relationships that could have appeared to influence the work reported in this paper.

Acknowledgments

The authors acknowledge the support by the RADIATE project under the Grant Agreement 824096 from the EU Research and Innovation programme HORIZON 2020. The VERA team acknowledges financial support of the ILIAMS research activities by “Investitionsprojekte” of the University of Vienna. We thank Toni Wallner for the chance to measure a series of low-level materials with the new setup.

References

[1] M. Basunia, A. Hurst, Nuclear data sheets for A = 26, Nucl. Data Sheets 134 (2016) 1–148.
[2] P. Steier, R. Golser, W. Kutschera, A. Priller, C. Vockenhuber, S. Winkler, VERA, an AMS facility for “all” isotopes, Nucl. Instrum. Methods B 223–224 (2004) 67–71.
[3] G. Rugel, S. Pavetich, S. Akhmadaliev, S.M.E. Baez, A. Scharf, R. Ziegenrücker, S. Merchel, The first four years of the AMS-facility DREAMS: status and developments for more accurate radionuclide data, Nucl. Instrum. Methods B 370 (2016) 94–100.
[4] M. Scheer, R.C. Bilodeau, J. Thøgersen, H.K. Haugen, Threshold photodetachment of Al^-: electron affinity and fine structure, Phys. Rev. A 57 (1998) R1493–R1496.
[5] M. Auer, W. Kutschera, A. Priller, D. Wagenbach, A. Wallner, E. Wild, Measurement of ^{26}Al for atmospheric and climate research and the potential of ^{26}Al/^{10}Be ratios, Nucl. Instrum. Methods B 259 (1) (2007) 595–599.
[6] M. Roberts, G. Bench, T. Brown, M. Caffee, R. Finkel, S. Freeman, L. Hainsworth, M. Kashgarian, J. McAninch, I. Proctor, J. Southon, J. Vogel, The LLNL AMS facility, Nucl. Instrum. Methods B 123 (1) (1997) 57–61.
[7] S. Xu, S.P. Freeman, D.H. Rood, R.P. Shanks, Decadal ^{10}Be, ^{26}Al and ^{36}Cl QA measurements on the SUERC 5MV accelerator mass spectrometer, Nucl. Instrum. Methods B 361 (2015) 39–42.
[8] S.R. Desai, H. Wu, L.-S. Wang, Vibrationally resolved photoelectron spectroscopy of AlO^- and AlO_2^-, Int. J. Mass Spectrom. 159 (1) (1996) 75–80.
[9] M. Gutowski, P. Skurski, X. Li, L.-S. Wang, $(MgO)_n^-$(n=1–5), Phys. Rev. Lett. 85 (2000) 3145–3148.
[10] A. Hunt, G. Petrucci, P. Bierman, R. Finkel, Investigation of metal matrix systems for cosmogenic ^{26}Al analysis by accelerator mass spectrometry, Nucl. Instrum. Methods B 260 (2) (2007) 633–636.
[11] J. Barker, J. Day, T. Aitken, T. Charlesworth, R. Cunningham, P. Drumm, J. Lilley, G. Newton, M. Smithson, Development of ^{26}Al accelerator mass spectrometry for biological and toxicological applications, Nucl. Instrum. Methods B 52 (3) (1990) 540–543.
[12] H. Faestermann, K. Kato, G. Korschinek, P. Krauthan, E. Nolte, W. Rühm, L. Zerle, Accelerator mass spectrometry with fully stripped ^{26}Al, ^{36}Cl, ^{41}Ca and ^{59}Ni ions, Nucl. Instrum. Methods B 50 (1) (1990) 275–279.
[13] A. Arazi, T. Faestermann, J.F. Niello, D. Frischke, K. Knie, G. Korschinek, H. Maier, E. Richter, G. Rugel, A. Wallner, Magnesium suppression for ^{26}Al measurements using AlO^- ions, Nucl. Instrum. Methods B 223–224 (2004) 259–262.
[14] L. Fifield, S. Tims, L. Gladkis, C. Morton, ^{26}Al measurements with ^{10}Be counting statistics, Nucl. Instrum. Methods B 259 (1) (2007) 178–183.
[15] K.-U. Miltenberger, A.M. Müller, M. Suter, H.-A. Synal, C. Vockenhuber, Accelerator mass spectrometry of ^{26}Al at 6MV using AlO- ions and a gas-filled magnet, Nucl. Instrum. Methods B 406 (2017) 272–277.
[16] M. Martschini, J. Pitters, T. Moreau, P. Andersson, O. Forstner, D. Hanstorp, J. Lachner, Y. Liu, A. Priller, P. Steier, R. Golser, Selective laser photodetachment of intense atomic and molecular negative ion beams with the ILIAS RFQ ion beam cooler, Int. J. Mass Spectrom. 415 (2017) 9–17.
[17] O. Forstner, P. Andersson, D. Hanstorp, J. Lahner, M. Martschini, J. Pitters, A. Priller, P. Steier, R. Golser, The ILIAS project for selective isobar suppression by laser photodetachment, Nucl. Instrum. Methods B 361 (2015) 217–221.
[18] M. Martschini, D. Hanstorp, J. Lachner, C. Marek, A. Priller, P. Steier, P. Wasserburger, R. Golser, The ILIAMS project – an RFQ ion beam cooler for selective laser photodetachment at VERA, Nucl. Instrum. Methods B 456 (2019) 213–217.
[19] J. Lachner, C. Marek, M. Martschini, A. Priller, P. Steier, R. Golser, ^{36}Cl in a new light: AMS measurements assisted by ion-laser interaction, Nucl. Instrum. Methods B 456 (2019) 163–168.
[20] O. Forstner, L. Michlmayr, M. Auer, R. Golser, W. Kutschera, A. Priller, P. Steier, A. Wallner, Applications of a compact ionization chamber in AMS at energies below 1 MeV/amu, Nucl. Instrum. Methods B 266 (10) (2008) 2213–2216.
[21] J.C. Rienstra-Kiracofe, G.S. Tschumper, H.F. Schaefer, S. Nandi, G.B. Ellison, Atomic and molecular electron affinities: photoelectron experiments and theoretical computations, Chem. Rev. 102 (1) (2002) 231–282. PMID: 11782134.
[22] H. Lischka, R. Shepard, R.M. Pitzer, I. Shavitt, M. Dallos, T. Müller, P.G. Szalay, M. Seth, G.S. Kedziora, S. Yabushita, Z. Zhang, High-level multireference methods in the quantum-chemistry program system COLUMBUS: analytic MR-CISD and MR-AQCC gradients and MR-AQCC-LRT for excited states, GUGA spin–orbit CI and parallel CI density, Phys. Chem. Chem. Phys. 3 (2001) 664–673.
[23] H. Lischka, R. Shepard, T. Müller, P.G. Szalay, R.M. Pitzer, A.J.A. Aquino, M.M. Araújo do Nascimento, M. Barbatti, L.T. Belcher, J.-P. Blaudeau, I. Borges, S.R. Brozell, E.A. Carter, A. Das, G. Gidofalvi, L. González, W.L. Hase, G. Kedziora, M. Kertesz, F. Kossoski, F.B.C. Machado, S. Matsika, S.A. do Monte, D. Nachtigallová, R. Nieman, M. Oppel, C.A. Parish, F. Plasser, R.F.K. Spada, E.A. Stahlberg, E. Ventura, D.R. Yarkony, Z. Zhang, The generality of the GUGA MRCI approach in COLUMBUS for treating complex quantum chemistry, J. Chem. Phys. 152 (13) (2020) 134110.
[24] J.A. Pople, R. Seeger, R. Krishnan, Variational configuration interaction methods and comparison with perturbation theory, Int. J. Quant. Chem. 12 (S11) (1977) 149–163.
[25] P. Widmark, P. Malmqvist, B. Roos, Density matrix averaged atomic natural orbital (ano) basis sets for correlated molecular wave functions, Theor. Chim. Acta 77 (1990) 291–306.
[26] H. Lischka, T. Müller, P.G. Szalay, I. Shavitt, R.M. Pitzer, R. Shepard, Columbus—a program system for advanced multireference theory calculations, WIREs Comput. Mol. Sc. 1 (2) (2011) 191–199.
[27] H. Lischka, R. Shepard, I. Shavitt, R.M. Pitzer, M. Dallos, T. Müller, P.G. Szalay, F.B. Brown, R. Ahlrichs, H.J. Böhm, A. Chang, D.C. Comeau, R. Gdanitz, H. Dachsel, C. Ehrhardt, M. Ernzerhof, P. Höchtl, S. Irle, G. Kedziora, T. Kovar, V. Parasuk, M.J.M. Pepper, P. Scharf, H. Schiffer, M. Schindler, M. Schüler, M. Seth, E.A. Stahlberg, J.-G. Zhao, S. Yabushita, Z. Zhang, M. Barbatti, S. Matsika, M. Schuurmann, D.R. Yarkony, S.R. Brozell, E.V. Blaudeau, B. J-P, M. Ruckenbauer, B. Sellner, F. Plasser, J.J. Szymczak, R.F.K. Spada, A. Das, Columbus, an Ab Initio Electronic Structure Program, Release 7.0, 2016.
[28] F. Aquilante, J. Autschbach, R.K. Carlson, L.F. Chibotaru, M.G. Delcey, L. De Vico, I.Fdez Galván, N. Ferré, L.M. Frutos, L. Gagliardi, M. Garavelli, A. Giussani, C.E. Hoyer, G. Li Manni, H. Lischka, D. Ma, P.A. Malmqvist, T. Müller, A. Nenov, M. Olivucci, T.B. Pedersen, D. Peng, F. Plasser, B. Pritchard, M. Reiher, I. Rivalta, I. Schapiro, J. Segarra-Martí, M. Stenrup, D.G. Truhlar, L. Ungur, A. Valentini, S. Vancoillie, V. Veryazov, V.P. Vysotskiy, O. Weingart, F. Zapata, R. Lindh, Molcas 8: new capabilities for multiconfigurational quantum chemical calculations across the periodic table, J. Comput. Chem. 37 (5) (2016) 506–541.
[29] S. Jacob, M. Suter, H.-A. Synal, Ion beam interaction with stripper gas - key for AMS at sub MeV, Nucl. Instrum. Methods B 172 (2000) 235–241.
[30] H.-J. Zhai, L.-M. Wang, S.-D. Li, L.-S. Wang, Vibrationally resolved photoelectron spectroscopy of BO^- and BO_2^-: a joint experimental and theoretical study, J. Phys. Chem. 111 (6) (2007) 1030–1035.
[31] V. Zengin, B. Joakim Persson, K.M. Strong, R.E. Continetti, Study of the low–lying electronic states of CCO by photoelectron spectroscopy of CCO^- and ab initio calculations, J. Chem. Phys. 105 (22) (1996) 9740–9747.
[32] J.M. Oakes, M.E. Jones, V.M. Bierbaum, G.B. Ellison, Photoelectron spectroscopy of anions from CCO^- and $HCCO^-$, J. Phys. Chem.-US 87 (24) (1983) 4810–4815.
[33] P. Steier, M. Martschini, J. Buchriegler, J. Feige, J. Lachner, S. Merchel, L. Michlmayr, A. Priller, G. Rugel, E. Schmidt, A. Wallner, E.M. Wild, R. Golser, Comparison of methods for the detection of ^{10}Be with AMS and a new approach based on a silicon nitride foil stack, Int. J. Mass Spectrom. 444 (2019) 116175.

[34] J. Lachner, M. Christl, A.M. Müller, M. Suter, H.-A. Synal, ^{10}Be and ^{26}Al low-energy AMS using He-stripping and background suppression via an absorber, Nucl. Instrum. Methods B 331 (2014) 209–214.
[35] A.M. Müller, M. Christl, J. Lachner, H.-A. Synal, C. Vockenhuber, C. Zanella, ^{26}Al measurements below 500kV in charge state 2+, Nucl. Instrum. Methods B 361 (2015) 257–262.
[36] M. Stocker, M. Döbeli, M. Grajcar, M. Suter, H.-A. Synal, L. Wacker, A universal and competitive compact AMS facility, Nucl. Instrum. Methods B 240 (1) (2005) 483–489.